Geophysical Prospecting **40**, 195–209, 1992

SHEAR-WAVE VELOCITY ESTIMATION IN POROUS ROCKS: THEORETICAL FORMULATION, PRELIMINARY VERIFICATION AND APPLICATIONS[1]

M. L. GREENBERG[2] and J. P. CASTAGNA[3]

ABSTRACT

GREENBERG, M.L. and CASTAGNA, J.P. 1992. Shear-wave velocity estimation in porous rocks: theoretical formulation, preliminary verification and applications. *Geophysical Prospecting* **40**, 195–209.

Shear-wave velocity logs are useful for various seismic interpretation applications, including bright spot analyses, amplitude-versus-offset analyses and multicomponent seismic interpretations. Measured shear-wave velocity logs are, however, often unavailable.

We developed a general method to predict shear-wave velocity in porous rocks. If reliable compressional-wave velocity, lithology, porosity and water saturation data are available, the precision and accuracy of shear-wave velocity prediction are 9% and 3%, respectively. The success of our method depends on: (1) robust relationships between compressional- and shear-wave velocities for water-saturated, pure, porous lithologies; (2) nearly linear mixing laws for solid rock constituents; (3) first-order applicability of the Biot–Gassmann theory to real rocks.

We verified these concepts with laboratory measurements and full waveform sonic logs. Shear-wave velocities estimated by our method can improve formation evaluation. Our method has been successfully tested with data from several locations.

INTRODUCTION

Explanations for porous rock response to elastic waves require knowledge of shear-wave velocity, yet data are often unavailable. Elastic wave theories (e.g. Kuster and Toksöz 1974; O'Connell and Budiansky 1974) that predict velocities invoke numerous simplifications which cannot account for the diversity of sedimentary rocks. A combination of empirical relations and robust aspects of theoretical model are required if a generalized method for predicting shear-wave velocity is to be successful.

While many empirical studies have focused on predicting velocities from porosity

[1] Received April 1991, revision accepted September 1991.
[2] Atlantic Richfield Corp., Plano, TX, U.S.A.
[3] ARCO Oil and Gas Company, Houston, TX, U.S.A.

and rock composition, these have necessarily had limited success, because velocity also depends on effective stress, porous rock structure (pore shape distribution) and degree of lithification. An alternative approach to shear-wave velocity prediction exists, because these factors affect compressional- and shear-wave velocity in a similar way and because compressional-wave velocity data are widely available. We have investigated the use of measured compressional-wave velocity, with porosity and lithology data, to predict shear-wave velocity.

Relationships between compressional- and shear-wave velocities are well-known for brine-saturated, pure lithologies (Pickett 1963). These relations are readily applied to mixed lithologies because, as predicted from Hashin and Shtrikman (1963) bounds, the solid rock constituents combine almost linearly.

A general method for shear-wave velocity prediction must account for rocks which are not brine saturated. Biot's (1956) theoretical work on elastic-wave propagation in porous media, once coupled to measurable elastic parameters by Geertsma and Smit (1961), showed that Gassmann's (1951) equations are generally applicable to statistically isotropic, porous rocks in the limit of zero-frequency wave propagation. When applied to real rocks, Gassmann's equations yield a first-order prediction for the dependence of elastic velocities on the properties of pore-filling fluids (e.g. Castagna, Batzle and Eastwood 1985).

We developed a method for predicting shear-wave velocity in porous, sedimentary rocks which couples empirical relations between shear- and compressional-wave velocities with Gassmann's equations. Mixed lithologies and fluids are accounted for. Laboratory measurements are used for method verification. We find that the mean predicted shear-wave velocity precision (2 standard deviations) is 9% and the accuracy is better than 3%. We provide preliminary verification of our technique using well log data. Shear-wave velocity errors in well log applications are found to be comparable to laboratory results.

Method for Estimating Shear-Wave Velocity

Development of coupled equations

Empirical relations between body shear-wave velocity β_i and compressional-wave velocity α_i in brine-filled rocks of pure (monomineralic) lithology have been adequately represented by polynomials (e.g. Castagna, Batzle and Kan 1992). Shear-wave velocity β_C in a homogeneous composite (multimineralic) brine-filled rock, can be approximated by averaging the harmonic and arithmetic means of the constituent pure porous-lithology shear-wave velocities. This averaging is analogous to obtaining a Voigt–Reuss–Hill average for the elastic moduli. For a homogeneous composite with compressional-wave velocity α_C, the porosity can be partitioned among L constituents such that $\alpha_1 \sim \alpha_2 \sim \cdots \sim \alpha_L \sim \alpha_C$. This partitioning approximation improves as the porosity increases or the constituent grain velocities converge. These observations specify an approximate relation between β_C and α_C for brine-filled rocks given by

$$\beta_C = 0.5\left(\left\{\sum_{i=0}^{L} X_i \sum_{j=0}^{N_i} a_{ij}\alpha_C^j\right\} + \left\{\sum_{i=0}^{L} X_i\left[\sum_{j=0}^{N_i} a_{ij}\alpha_C^j\right]^{-1}\right\}^{-1}\right), \qquad 1 = \sum_{i=0}^{L} X_i, \tag{1}$$

where α_C, β_C are the compressional- and shear-wave velocities, respectively, of a composite rock, L is the number of pure (monomineralic) porous constituents, X_i is the dry lithology volume fraction of lithological constituent i, a_{ij} are the empirical coefficients and $0 \leq N_i$ the order of polynomial i.

Gassmann (1951) obtained equations for a homogeneous isotropic rock relating α_C and β_C to the crystalline frame and the pore-fluid properties. The effects of varying the fluid saturation on α_C and β_C can be estimated (e.g. Domenico 1976) by combining Gassmann's equations, the mass balance for a composite rock density, and Wood's (1957) equation; the latter is applied to estimate the homogeneously mixed fluid incompressibility. By combining these equations with (1) and composite grain incompressibility, an estimation of β_C for rocks of mixed lithology at arbitrary brine saturation can be obtained.

For homogeneous, isotropic, linearly elastic media, the body-wave velocities are given by

$$\alpha_C^2 = (K_C + [4/3]\mu_C)/\rho_C \tag{2a}$$

and

$$\beta_C^2 = \mu_C/\rho_C \tag{2b}$$

where K_C is the incompressibility, μ_C is the shear modulus and ρ_C is the mass density. Gassmann's equations can be expressed as extensions of (2), relating K_C and μ_C to the frame, grain and pore-filling fluid properties (e.g. Domenico 1976). Thus

$$K_C = K_D + (\Gamma + \phi)^2/(\Gamma K_{gC}^{-1} + \phi K_{fC}^{-1}) \tag{3a}$$

and

$$\mu_C\{X, \phi, S_w\} = \mu_C\{X, \phi, 1\} = \mu_C\{X, \phi\}\ , \tag{3b}$$

where $\Gamma = (1 - \phi - K_D/K_{gC})$, and ϕ is the volume fraction of pore space (porosity), $\mathbf{X}$ is the vector of dry constituent mineral volume fractions, $\{X_i\}$, S_w is the volume fraction of pore space filled with brine, K_{gC} is the incompressibility of homogeneously mixed mineral grains, $K_D = K_D\{\mathbf{X}, \phi\}$ is the incompressibility of composite solid rock frame (skeleton) and K_{fC} is the incompressibility of homogeneously mixed pore-filling fluids.

The frame moduli K_D and μ_C are implicitly dependent on rock texture and degree of lithification and explicitly dependent on lithology and porosity.

For an arbitrary homogeneous mixture of pore-filling fluids and minerals, the mass balance, Wood's equation and the Voigt–Reuss–Hill estimate for mixed grain incompressibility, are respectively,

$$\rho_C = \phi(S_w\rho_w + [1 - S_w]\rho_{nw}) + (1 - \phi)\sum_{i=0}^{L} X_i\rho_i, \tag{4a}$$

$$K_{fC}^{-1} = S_w K_w^{-1} + (1 - S_w)K_{nw}^{-1}, \tag{4b}$$

$$K_{gC} = \left(\sum_{i=0}^{L} X_i K_i + \left[\sum_{i=0}^{L} X_i K_i^{-1}\right]^{-1}\right)\Big/2, \tag{4c}$$

where ρ_w and K_w are the brine mass density and incompressibility, respectively, ρ_{nw} and K_{nw} are the non-wetting fluid mass density and incompressibility, respectively, and ρ_i and K_i are the dry constituent i mass density and incompressibility, respectively.

Solution of coupled equations

In order to estimate the shear-wave velocity β_C for a rock with brine saturation S_w, (2)–(4) must be combined to give a brine-saturated compressional-wave velocity estimate so that (1) can be applied. Equation (1) estimates the brine-saturated shear-wave velocity, which is then related to the shear-wave velocity at S_w using (3b) and ratios obtained from (2b) and (4a). Measurements of the compressional-wave velocity α_C (typically at S_w), lithology, porosity and brine saturation are required, as are the specification of the constituent properties $\{a_{ij}, \rho_w, K_w, \rho_{nw}, K_{nw}, \rho_i, K_i\}$.

We developed an iterative method since an analytical solution is intractable. An iteration parametrization permitting a robust choice of starting model (seed) is required, as multiple solutions (mostly non-physical) exist. Since typical *in situ* variation of compressional-wave velocity with brine saturation is less than 20%, a scheme to optimize the difference between compressional-wave velocities at S_w and 100% brine saturation ($S_w = 1$) can be initiated.

Using subscript S to denote properties at brine saturation S_w and subscript 1 to denote properties at 100% brine saturation, we can write

$$\alpha_{1C} = (1 + \delta)\alpha_{SC}, \tag{5}$$

where δ is a slack variable with a probable optimal value in the range 0.0–0.2.

Combining (1)–(4) yields a second estimate of α_{1C} (α'_{1C} below), which can be compared with (5) to establish an iteration convergence criterion. α'_{1C} can be obtained in four steps (Fig. 1), provided (4a, b, c) are pre-evaluated at measured S_w and $S_w = 1$.

Step 1. Use (5) and apply (1) followed by (2b) at $S_w = 1$:

$$\mu_C = 0.25\rho_{1C}\left(\left\{\sum_{i=0}^{L} X_i \sum_{j=0}^{N_i} a_{ij}(1 + \delta)^j \alpha_{SC}^j\right\} + \left\{\sum_{i=0}^{L} X_i\left[\sum_{j=0}^{N_i} a_{ij}(1 + \delta)^j \alpha_{SC}^j\right]^{-1}\right\}^{-1}\right)^2.$$

Step 2. Apply (2a) and (3b) at S_w using μ_C from step 1:

$$K_{SC} = \rho_{SC}\alpha_{SC}^2 - (4/3)\mu_C.$$

Step 3. Solve (3a) for K_D and apply result at S_w using K_{SC} from step 2:

$$K_D = K_{gC}(\lambda K_{SC} - 1)/(\lambda K_{gC} - 2 + [K_{SC}/K_{gC}]),$$

where

$$\lambda = \phi K_{gC}^{-1} + (1 - \phi)K_{SfC}^{-1}.$$

Step 4. Apply (2a) and (3a) at $S_w = 1$ using μ_C from step 1 and K_D from step 3:

$$\alpha'_{1C} = \sqrt{\{(K_D + [4/3]\mu_C + [\Gamma + \phi]^2/[\Gamma K_{gC}^{-1} + \phi K_w^{-1}])/\rho_{1C}\}}.$$

When the measurements and the required shear-wave velocity are for 100% brine-saturated rock, $\delta = 0$ and iterations are unnecessary. In this case, steps 1, 2 and 3

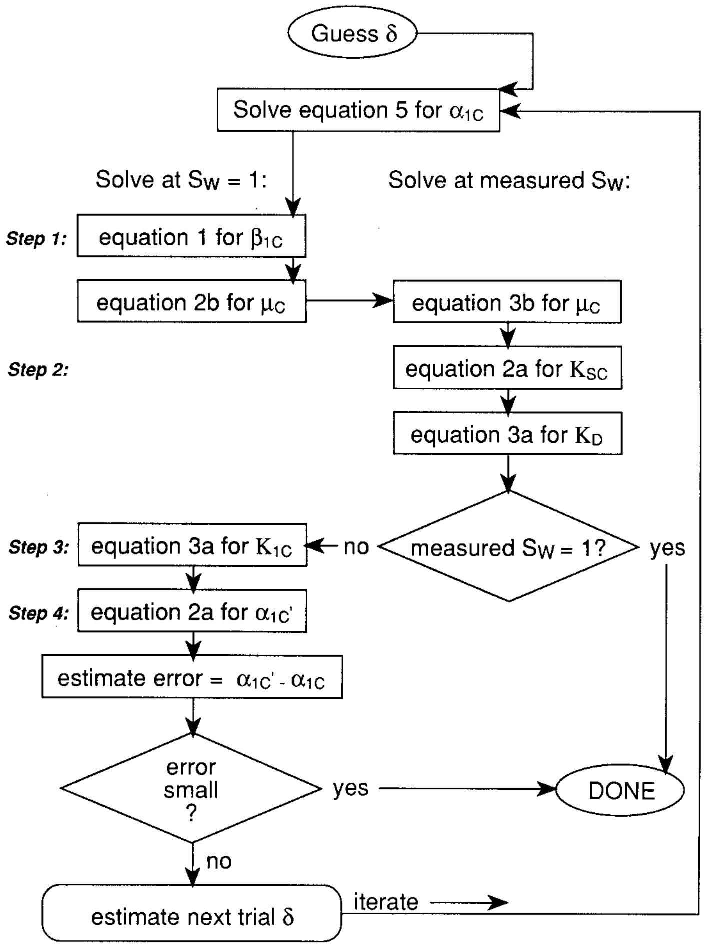

FIG. 1. Procedure for estimating shear-wave velocity, given measurements of compressional-wave velocity, lithology, porosity and fluid saturations. Constituent properties and $\alpha_C - \beta_C$ trend coefficients are required *a priori* (e.g. Tables 1 and 2 for grain properties; Batzle and Wang (1992) for fluid properties). Pre-evaluate equations 4 for $\{\rho_{1C}, \rho_{SC}, K_{1fC}, K_{SfC}, K_{gC}\}$. Nomenclature defined in text.

still may be followed to estimate the frame moduli, although (1) is sufficient to estimate β_{1C}.

Model Verification

We verified our model using laboratory and well log measurements of sedimentary rocks of quartz, calcite, dolomite and clay minerals. Clay is defined here as the dry mineral fraction of shale and is assumed to have the properties of illite.

TABLE 1. Representative regression coefficients for shear-wave velocity (β_C[km/s]) versus compressional-wave velocity (α_C, [km/s]) in pure porous lithologies: $\beta_C = a_{i2}\alpha_C^2 + a_{i1}\alpha_C + a_{i0}$ (Castagna *et al.* 1992).

Lithology	a_{i2}	a_{i1}	a_{i0}
Sandstone	0	0.80416	−0.85588
Limestone	−0.05508	1.01677	−1.03049
Dolomite	0	0.58321	−0.07775
Shale	0	0.76969	−0.86735

Our method for shear-wave velocity estimation requires *a priori* knowledge of the polynomial coefficients for pure porous lithology β_C versus α_C trends, and of the intrinsic mineral and fluid properties. Castagna *et al.* (1992) reported coefficients of ultrasonic β_C versus α_C polynomial regressions for sandstone, limestone, dolomite and shales (Table 1). Mineral mass density, compressional-wave velocity and shear-wave velocity were given by Carmichael (1989) for quartz and calcite, Anderson and Lieberman (1966) for dolomite, and Eastwood and Castagna (1986) for illite. Mineral incompressiblities are determined from mineral velocities, using (2) (Table 2). For most sedimentary basins, the dependence of intrinsic mineral properties on pressure and temperature is negligible.

We modelled pressure- and temperature-dependent properties of brine, methane and oil in the subsurface according to Batzle and Wang (1992). In our laboratory measurements of air-saturated rocks, the effects of extrinsic gas property dependence on shear-wave velocity estimations were not detectable. For modelling with laboratory data, we used constant properties for water (mass density = 1.0 g/cm^3 and incompressibility = 2.2 GPa) and nitrogen (mass density = 1.297×10^{-3} g/cm^3 and incompressibility = 1.417×10^{-4} GPa), the latter values are given by Domenico (1976).

TABLE 2. Intrinsic elastic properties of representative rock-forming minerals: mass density (ρ_g [g/cm^3]), compressional-wave velocity (α_g [km/s]), shear-wave velocity (β_g [km/s]) and incompressibility (K_g [GPa]).

Mineral	ρ_g (g/cm^3)	α_g (km/s)	β_g (km/s)	K_g (GPa)[1]
Quartz[2]	2.649	6.05	4.09	37.88
Calcite[2]	2.712	6.53	3.36	74.82
Dolomite[3]	2.87	7.05	4.16	76.42
Illite[4]	2.66	4.32	2.54	26.76

[1] Estimated from α_g, β_g and ρ_g using (2). [2] Carmichael (1989). [3] Anderson and Lieberman (1966). [4] Eastwood and Castagna (1986).

Verification with laboratory data

Shear-wave velocities were estimated and compared to laboratory measurements for sets of brine- and air-filled rocks. We incorporated data sets from Rafavich, Kendal and Todd (1984), Han, Nur and Morgan (1986) and Tosaya (1982) with our own. Only those sets with high-quality lithology, porosity, density, compressional- and shear-wave velocity data were selected. Errors in quantitative mineralogies were not uniform as volumetric data was acquired by X-ray diffraction in some cases and by point count on thin section in others. The mineralogy consisted principally of quartz, calcite and dolomite. Feldspar, when present, was modelled as clay. The combined clay and feldspar content did not exceed 3% of dry mineralogy by volume. The combined volumes of quartz, calcite, dolomite, clay and feldspar were not less than 95% of dry mineralogy; the neglected remainder was principally anhydrite for carbonate samples.

Laboratory velocity measurements were acquired by ultrasonic methods. All measurements were at ambient temperature. Confining pressures varied from 0 to 200 MPa and pore pressures varied from 0 to 170 MPa. Multiple velocity measurements on a rock at different pressures were treated as distinct data sets. For each sample, mineral densities were adjusted from values in Table 2 (on a mineral fraction volume-weighted basis) to satisfy the mass balance (4a).

The results of our shear-wave velocity estimation method are compared to measured shear-wave velocities in Figs 2 and 3 for water- and air-filled rocks, respectively. Characteristically, large errors in quantitative mineralogy analyses preclude the estimation of the model error; however, a combination of model and data error can be assessed from regression results. 93% of variance in 336 water-filled samples and 89% of variance in 341 air-filled samples are accounted for by our model, based on correlation coefficients.

The upper limit of the modelled shear-wave velocity precision is twice the estimated data variance shown in Figs 2 and 3. For water-filled rocks, the model shear-wave velocity variance is ± 83 m/s, whereas for air-filled rocks, ± 82 m/s. The mean fractional variance, within the range 2.2–3.8 km/s, is 0.045 for water- and air-filled rocks. The upper limit of precision is 9.0%.

We estimate model shear-wave velocity accuracy as the mean error determined from an estimated versus measured shear-wave velocity regression line. There is a small negative bias in the estimated shear-wave velocities of water- and air-filled rocks since both regression lines lie beneath the diagonal, over the range of measured shear-wave velocities. We estimate mean accuracies of 30 m/s and 62 m/s for water- and air-filled rocks, respectively, within the range 2.2–3.8 km/s. Mean fractional error, within the range 2.2–3.8 km/s, is 0.016 and 0.033 for water- and air-filled rocks, respectively. The overall accuracy is no worse than 3.3%.

Our statistical assessment of laboratory data modelling results indicates that shear-wave velocity estimation is robust. The estimated accuracy (3%) is substantially better than the estimated precision (9%), indicating that our method is unbiased. Combining ultrasonic β_C versus α_C plots with Gassmann's (1951) zero-frequency model appears to yield reasonable results when applied to ultrasonic data.

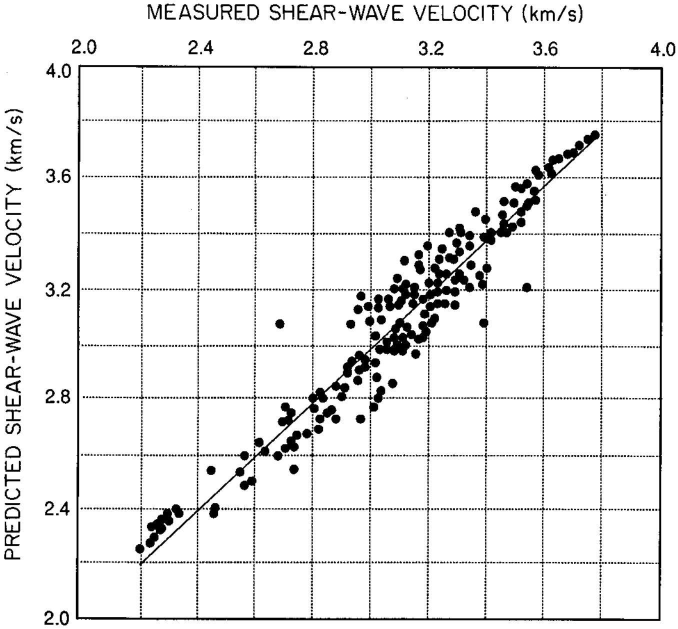

FIG. 2. Comparison of estimated shear-wave velocity ($\beta_{C(E)}$) with laboratory shear-wave velocity measurements ($\beta_{C(M)}$), in km/s, for water-filled rocks. No. samples: 336, least-squares regression: $\beta_{C(E)} = 0.9965\ \beta_{C(M)} - 0.0172$, variance: ± 83.6 m/s, correlation coefficient: $+0.9648$.

Laboratory results were derived from nearly shale-free rocks, due to inherent difficulties in laboratory work with shales.

Verification with well log data

Compressional- and shear-wave velocities are typically measured with well logging tools at about 10 kHz. In brine-saturated rocks, ultrasonic β_C versus α_C trends may be used to estimate β_C at well log frequencies because dispersion is negligible (Eastwood and Castagna 1986). In gas-saturated rocks, however, dispersion may be significant. A profile of decreasing drilling fluid saturation with radial distance from the borehole, often observed after drilling in initially gas-saturated rocks, can further complicate matters, because well logs do not all sample equivalent volumes of rock.

Empirically, complicating factors in gas-saturated rocks are difficult to separate. When our method for estimating shear-wave velocity was applied to well logs, we found good agreement with measured shear-wave sonic logs without an explicit dispersion correction. For seismic applications, a dispersion correction (Winkler 1986) may be desirable. We preferentially use a fluid saturation estimate derived from logs which sample a rock volume comparable to that sampled by sonic logs.

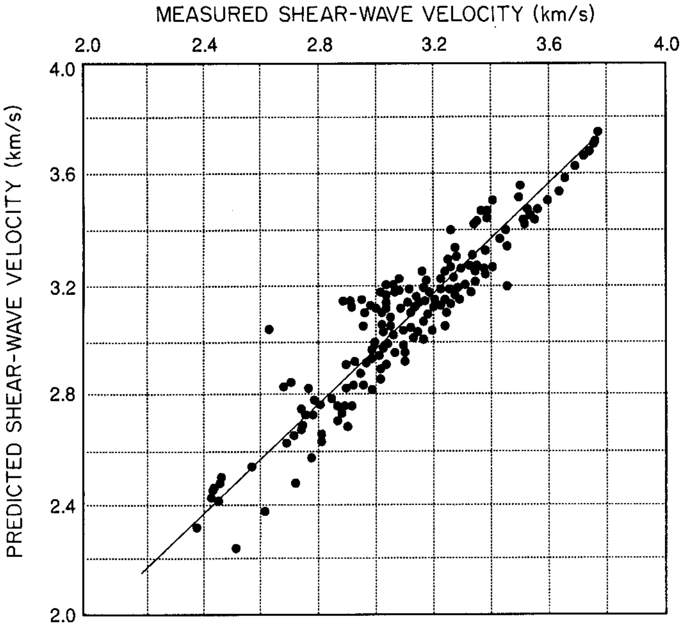

FIG. 3. Comparison of estimated shear-wave velocity ($\beta_{C(E)}$) with laboratory shear-wave velocity measurements ($\beta_{C(M)}$), in km/s, for air-filled rocks. No. samples: 341, least-squares regression: $\beta_{C(E)} = 0.9670\beta_{C(M)} + 0.0447$, variance: ± 86.7 m/s, correlation coefficient: $+0.9393$.

Example 1: South Texas clastics

A high-quality multichannel sonic waveform-derived shear-wave transit-time log (Aron, Murray and Seeman 1978, paper at 53rd SPE meeting, Houston) from South Texas is compared with the shear-wave velocity estimated by an approach comparable to the methodology described above (Fig. 4). The shear-wave velocity was initially estimated using lithology determined from a gamma ray log (assuming a linear response to shale volume) and the porosity estimated from density log data (assuming constant grain density). Large discrepancies between the estimated and measured shear-wave velocities led to a re-examination of the available log data which revealed high gamma count rates in relatively shale-free intervals, probably due to the presence of uranium. The lithology and porosity were subsequently re-estimated by inverting a linear system of equations representing the environmental response of sonic, neutron and density logs. The revised estimates of the shear-wave velocity agree closely with measurements (Fig. 4).

The semblance among array sonic log waveforms at each acquisition depth provides an indication of shear-wave log reliability (Siegfried and Castagna 1982, paper at 23rd meeting of the Society of Professional Well Log Analysts, Corpus Christi). Figure 5 shows the standard deviation of differences between estimated and measured shear-wave transit times, among data with similar (± 0.05) semblance, as a function of semblance for a 0.73 km interval (4800 data points) in the South Texas well. As the semblance approaches one (i.e. as the transit-time measurement quality

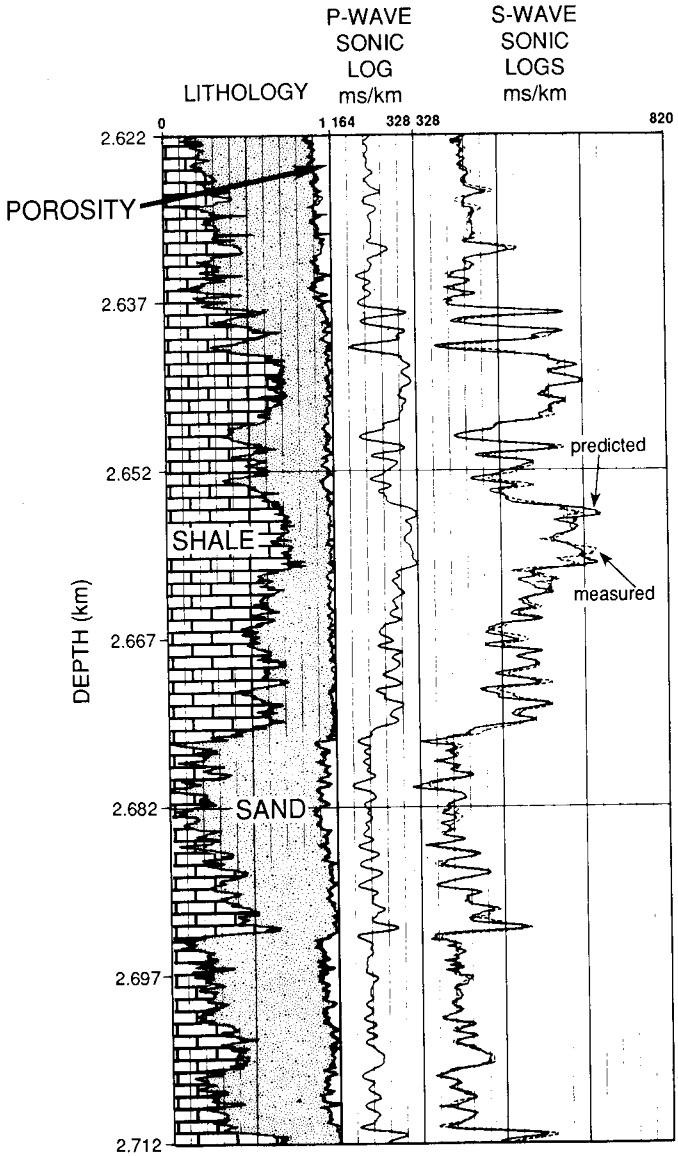

FIG. 4. South Texas clastics example. Lithology analysis and transit-time log measurements. Estimated shear-wave transit-time overlain on waveform-derived measured shear-wave transit time.

improves), the standard deviation of differences between estimated and measured shear-wave transit times approaches 11.5 ms/km. This limit is less than the standard deviation (19.7 ms/km) of repeated shear-wave transit times (using different logging instruments) observed by Castagna (1985, paper at 55th SEG meeting, Washington) in Gulf Coast clastics.

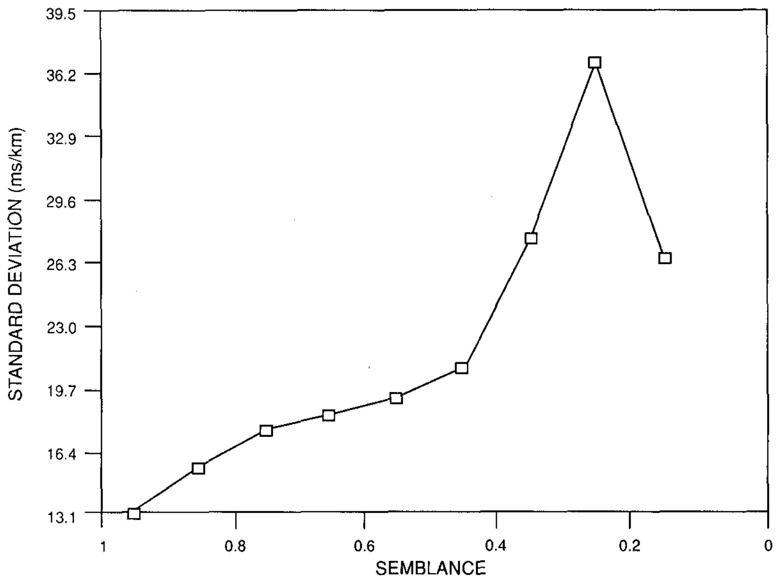

FIG. 5. Standard deviation of discrepancy between estimated and measured shear-wave transit-time, among data with similar (± 0.05) semblance, versus semblance for the South Texas clastics example.

Using the mean observed shear-wave transit time (311.7 ms/km) and the limiting error at perfect semblance ($\sigma = 11.5$ ms/km), the estimated shear-wave transit-time precision (2σ) is about 7% for the South Texas clastics well. Since measurement precision at perfect semblance is finite, the precision due to prediction methodology may be significantly better than 7%. The estimated shear-wave velocity precision for this example is better than the precision obtained from laboratory data (9%).

Example 2: Offshore Gulf of Mexico clastics

Dipole-source waveform-derived shear-wave logging tool feasibility was demonstrated by Zemanek *et al.* (1984, paper at 25th meeting of the Society of Professional Well Log Analysts, New Orleans). Shear-wave transit times, predicted by an approach comparable to the methodology described above, are compared with dipole tool shear-wave transit-time data from an offshore Louisiana well in Fig. 6. The presented data are 0.6 m vertical averages spanning 0.3 km of shale, brine-saturated sandstone and gas-bearing sandstone.

Errors in the shear-wave transit-time prediction were assessed using the methods described above for laboratory data. Precision and accuracy estimates derived from the data shown in Fig. 6 were 9.0% and +2.7%, respectively. 81% of data variance was accounted for by our model, based on the correlation coefficient. Statistical results for this well were substantially better than those obtained by comparing our model with laboratory data.

Data from a second dipole-source shear-wave logging tool, taken over the interval shown in Fig. 6, are compared with the first dipole-source shear-wave logging

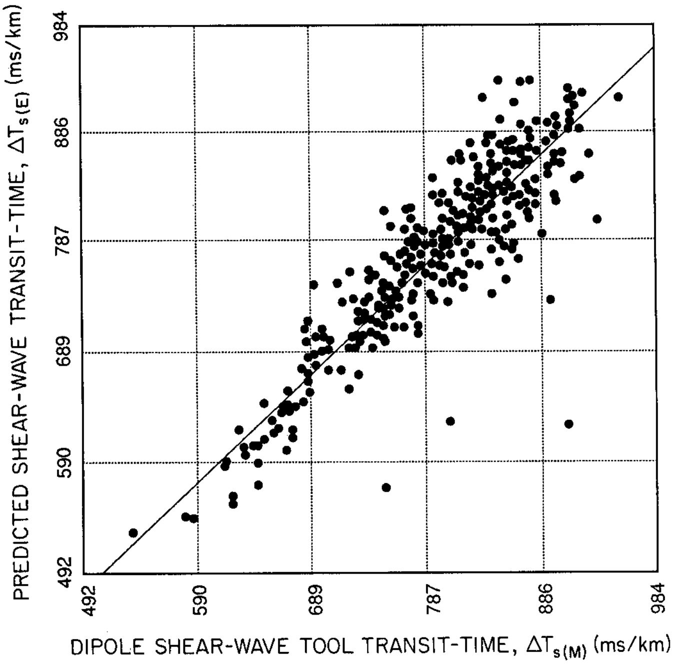

FIG. 6. Offshore Gulf of Mexico example. Predicted shear-wave transit-time ($\Delta T_{S(E)}$ [ms/km]) versus dipole sonic tool shear-wave transit-time ($\Delta T_{S(M)}$ [ms/km]) data, spanning a 0.3 km vertical section. Data are 0.6 m vertical averages. No. samples: 500, least-squares regression: $\Delta T_{S(E)} = 0.9831 \Delta T_{S(M)} - 7.46$, variance: ± 32.3 ms/km, correlation coefficient: $+0.9005$.

tool data (abscissa) in Fig. 7. Although similar principles were applied, the tools were built by different companies. Data scatter in Figs 6 and 7 are comparable. Estimates of precision and accuracy for the second tool, treating data from the first tool as error-free, are 9.3% and −2.4%, respectively. 76% of data variance was accounted for by linear regression, based on the correlation coefficient. Our method for shear-wave transit-time estimation yielded results as close to the measured dipole shear-wave logging tool data as were obtained with a second tool.

DISCUSSION

Combining Gassmann's (1951) equations and empirical α_C–β_C trends yields estimates for K_D and μ. Approximate equivalence of K_D and μ for sandstones, assumed by Castagna *et al.* (1985), is not required, and frame softening is accounted for implicitly.

Reliance on α_C–β_C trends is perhaps the greatest strength of our method, because these trends fit a broad class of real rocks empirically. Although our method could be extended by incorporating velocity–porosity relations, tend to vary with rock type and between sedimentary basins. Porosity information is usually available

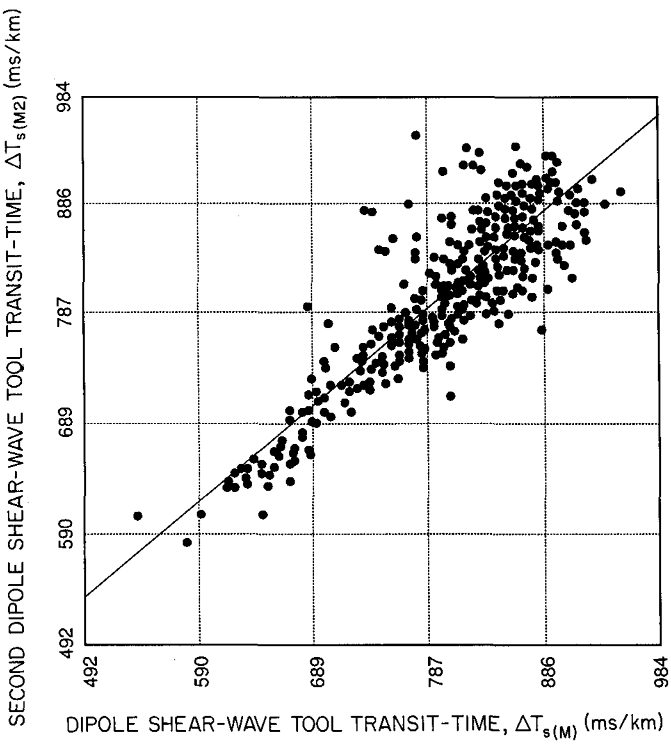

FIG. 7. Offshore Gulf of Mexico example: Second dipole sonic tool shear-wave transit-time ($\Delta T_{S(M2)}$ [ms/km]) versus the dipole sonic tool shear-wave transit-time ($\Delta T_{S(M)}$ [ms/km]) data shown in Fig. 6. Data are 0.6 m vertical averages. No. samples: 501, least-squares regression: $\Delta T_{S(M2)} = 0.8750\ \Delta T_{S(M)} + 104.4$, variance: ± 33.5 ms/km, correlation coefficient: $+0.8711$.

where essential for shear-wave velocity estimation (partially saturated rocks), because it is required for hydrocarbon resource assessment. For the majority of geophysically important, non-reservoir rocks, only α_C and their lithology are required to estimate shear-wave velocity. While porosity is used explicitly in our coupled equations, porosity, rock structure and lithification dependence of K_D and μ are contained implicitly in α_C data. For these reasons, our method neither assumes nor predicts relations between elastic velocities and porosity.

Our method also implies nothing about relations between elastic velocities and lithology, since lithology changes are usually accompanied by structural changes in a porous rock. The dependence of elastic velocities on pore fluid composition can be estimated with our approach because that dependence is modelled explicitly in Biot–Gassmann theory, provided that the constituent fluid properties are known and that the composite fluid remains homogeneously mixed.

Predicted shear-wave velocities serve to check data consistency and to identify anomalous rock properties when lithology, porosity, fluid saturation, α_C and β_C are all available from well log measurements. Predicted shear-wave velocities can help identify intervals where measured shear-wave velocity logs require correction. Our method has proved valuable for analyses of shallow sediments from well logs, because full waveform sonic logs do not detect shear-wave arrivals in unconsolidated sediments, and direct shear-wave logging tools have only recently become available.

To the first order, α_C–β_C trends are independent of pressure. Pressure effects on shear-wave velocities are implicitly accounted for in our method by using α_C–β_C trends. Measured α_C increases with effective stress and estimated β_C increases due to dependence on α_C.

Errors estimates provided here are upper limits due to significant errors in lithology analyses and errors in measured velocities (both α_C and β_C).

Conclusions

We have developed a technique for predicting shear-wave velocity from compressional-wave velocity and rock composition data. Our method couples robust empirical relations between compressional- and shear-wave velocities in brine-saturated rocks with a theoretical model (Gassmann 1951) for estimating the dependence of velocity on fluid composition. Tests conducted with laboratory and well log data indicate that shear-wave velocity can be estimated with a precision of better than 7%.

Acknowledgements

We thank ARCO Oil and Gas Company for permission to publish this paper. We are indebted to M. L. Batzle, F. P. Filice and K. W. Tubman for supplying the shear-wave velocity measurements and we thank M. V. Popa and R. L. Phillips for their many contributions to this work.

References

Anderson, O.L. and Lieberman, R.C. 1966. Sound velocities in rocks and minerals. VESIAC state-of-the-art report no. 7885-4-X. University of Michigan.

Batzle, M.L. and Wang, Z. 1992. Seismic properties of pore fluids. In: *Offset-Dependent Reflectivity*. J. P. Castagna and M. M. Backus (eds), Society of Exploration Geophysics, in press.

Biot, M.A. 1956. Theory of propagation of elastic waves in a fluid-saturated porous solid. I. Low-frequency range. *Journal of the Acoustical Society of America* **28**, 168–178.

Carmichael, R.S. (ed). 1989. CRC Practical Handbook of Physical Properties of Rocks and Minerals. CRC Press, Inc., Boca Raton, Florida, USA, 741 pages.

Castagna, J.P., Batzle, M.L. and Eastwood, R.L. 1985. Relationships between compressional-wave and shear-wave velocities in clastic silicate rocks. *Geophysics* **50**, 571–581.

Castagna, J.P., Batzle, M.L. and Kan, T.K. 1992. Rock physics: The link between rock properties and amplitude-versus-offset response In: *Offset-Dependent Reflectivity*. J. P. Castagna and M. M. Backus (eds), Society of Exploration Geophysics, in press.

DOMENICO, S.N. 1976. Effect of brine–gas mixture on velocity in an unconsolidated sand reservoir. *Geophysics* **41**, 882–894.

EASTWOOD, R.L. and CASTAGNA, J.P. 1986. Interpretation of V_p/V_s ratios from sonic logs. In: *Shear Wave Exploration*. S. H. Danbom and S. N. Domenico (eds), Geophysical Developments No. 1, Society of Exploration Geophysicists.

GASSMANN, F. 1951. Ueber die Elastizität poröser Medien *Vierteljahrschrift der Naturforschenden Gesellschaft, Zürich* **96**, 1–22.

GEERTSMA, J. and SMIT, D.C. 1961. Some aspects of elastic wave propagation in fluid saturated porous solids. *Geophysics* **26**, 169–181.

HAN, DE-HAU, NUR, A. and MORGAN, D. 1986. Effects of porosity and clay content on wave velocities in sandstones. *Geophysics* **51**, 2093–2107.

HASHIN, Z. and SHTRIKMAN, S. 1963. Variational approach of the theory of the elastic behavior of multiphase materials. *Journal of the Mechanics and Physics of Solids* **11**, 127–140.

KUSTER, G.T. and TOKSÖZ, M.N. 1974. Velocity and attenuation of seismic waves in two phase media: Part 1. Theoretical formulations. *Geophysics* **39**, 587–606.

MURPHY, W.F. 1982. Effects of microstructure and pore fluids on acoustic properties of granular sedimentary materials. Ph.D. thesis, Stanford University.

O'CONNELL, R.J. and BUDIANSKY, B. 1974. Seismic velocities in dry and saturated cracked solids. *Journal of Geophysical Research*, **79**, 5412–5426.

PICKETT, G.R. 1963. Acoustic character logs and their applications in formation evaluation. *Journal of Petroleum Technology* **15**, 650–667.

RAFAVICH, F., KENDAL, C.H.St.C. and TODD, T.P. 1984. The relationship between acoustic properties and the petrographic character of carbonate rocks. *Geophysics* **49**, 1622–1636.

TOSAYA, C.A. 1982. Acoustical properties of clay-bearing rocks. Ph.D. thesis, Stanford University.

WINKLER, K.W. 1986. Estimates of velocity dispersion between seismic and ultrasonic frequencies. *Geophysics* **51**, 183–189.

WOOD, A.B. 1957. *Textbook of Sound; Being an Account of the Physics of Vibrations with Special Reference to Recent Theoretical and Technical Developments*. Neil & Co. Ltd, Edinburgh, 610 pages.